

BRL CR 321

# BRL

AD A032444

CONTRACT REPORT NO. 321

PHOTODISSOCIATION SPECTROSCOPY  
OF  $\text{CO}_3^{*-}$

CIRCULATING COPY  
22 NOV 1996

Prepared by

Stanford Research Institute  
Menlo Park, California 94025

PROPERTY OF U.S. ARMY  
STINFO BRANCH  
BRL, APG, MD. 21005

November 1976

Approved for public release; distribution unlimited.

USA BALLISTIC RESEARCH LABORATORIES  
ABERDEEN PROVING GROUND, MARYLAND

Destroy this report when it is no longer needed.  
Do not return it to the originator.

Secondary distribution of this report by originating  
or sponsoring activity is prohibited.

Additional copies of this report may be obtained  
from the National Technical Information Service,  
U.S. Department of Commerce, Springfield, Virginia  
22151.

The findings in this report are not to be construed as  
an official Department of the Army position, unless  
so designated by other authorized documents.

UNCLASSIFIED

SECURITY CLASSIFICATION OF THIS PAGE (When Data Entered)

REPORT DOCUMENTATION PAGE		READ INSTRUCTIONS BEFORE COMPLETING FORM
1. REPORT NUMBER  CONTRACT REPORT NO. 321	2. GOVT ACCESSION NO.	3. RECIPIENT'S CATALOG NUMBER
4. TITLE (and Subtitle)  PHOTODISSOCIATION SPECTROSCOPY OF CO <sub>3</sub> <sup>-*</sup>		5. TYPE OF REPORT & PERIOD COVERED Interim Report 1 Jan - 31 Dec 75
		6. PERFORMING ORG. REPORT NUMBER
7. AUTHOR(s)  J. T. Moseley, P. C. Cosby, and J. R. Peterson		8. CONTRACT OR GRANT NUMBER(s)  DA-HC04-73-C-0016
9. PERFORMING ORGANIZATION NAME AND ADDRESS Stanford Research Institute Menlo Park, California 94025		10. PROGRAM ELEMENT, PROJECT, TASK AREA & WORK UNIT NUMBERS  RDT&E 1T162111AH71-A4 & RDT&E 1T161102B53A
11. CONTROLLING OFFICE NAME AND ADDRESS US Army Ballistic Research Laboratory Aberdeen Proving Ground, Maryland 21005		12. REPORT DATE NOVEMBER 1976
		13. NUMBER OF PAGES 30
14. MONITORING AGENCY NAME & ADDRESS (if different from Controlling Office) US Army Materiel Development & Readiness Command 5001 Eisenhower Avenue Alexandria, Virginia 22333		15. SECURITY CLASS. (of this report)  Unclassified
		15a. DECLASSIFICATION/DOWNGRADING SCHEDULE
16. DISTRIBUTION STATEMENT (of this Report)  Approved for public release; distribution unlimited.		
17. DISTRIBUTION STATEMENT (of the abstract entered in Block 20, if different from Report)		
18. SUPPLEMENTARY NOTES  PROPERTY OF U.S. ARMY STINFO BRANCH BRL, APG, MD. 21005		
19. KEY WORDS (Continue on reverse side if necessary and identify by block number) Photodissociation                      Carbon Trioxide Ion Photodetachment                      Reaction Rates Negative Ions                              Atmospheric Chemistry Lasers		
20. ABSTRACT (Continue on reverse side if necessary and identify by block number) (eal) The photodissociation cross section of the carbon trioxide negative ion has been measured over the wavelength range from 457.9 nm to 694.0 nm, and reveals detailed structure reflecting the vibrational spacings of the predissociating excited electronic state. From an analysis of the structure, we identified three vibrational modes of the excited state having energies of 990 cm(-1), 1470 cm(-1), and 880 cm(-1). The bond energy of the carbon trioxide negative ion (to separation into a carbon dioxide molecule and an atomic oxygen negative ion) was		

UNCLASSIFIED

SECURITY CLASSIFICATION OF THIS PAGE(When Data Entered)

Item 20 (Contd).

determined to be  $1.8 \pm 0.1$  eV, and the electron affinity of carbon trioxide was found to be  $2.9 \pm 0.3$  eV. By comparison with theoretical calculations, the lowest predissociating state was identified as the one doublet A one state. Observations regarding other excited states of the carbon trioxide negative ion are made.

UNCLASSIFIED

SECURITY CLASSIFICATION OF THIS PAGE(When Data Entered)

## TABLE OF CONTENTS

	Page
I. INTRODUCTION . . . . .	5
II. PHOTODISSOCIATION SPECTRUM . . . . .	6
III. VIBRATIONAL FREQUENCIES OF THE EXCITED STATE . . . . .	11
IV. IDENTIFICATION OF THE EXCITED STATE. . . . .	16
V. OTHER OBSERVATIONS . . . . .	20
VI. BOND ENERGY AND ELECTRON AFFINITY. . . . .	22
VII. SUMMARY. . . . .	23
ACKNOWLEDGEMENTS . . . . .	24
REFERENCES . . . . .	25
DISTRIBUTION LIST. . . . .	27



## I. INTRODUCTION

The negative ion  $\text{CO}_3^-$  is believed to be important in the ion chemistry of the D region<sup>1,2</sup> of the ionosphere and in  $\text{CO}_2$  lasers.<sup>3</sup> This ion has been studied in the solid state both in  $\text{KHCO}_3$  crystals<sup>4-6</sup> and in an argon matrix.<sup>7</sup> Walsh,<sup>8</sup> in his classic series of papers on molecular geometry, discussed the expected electron configuration and geometry of  $\text{CO}_3^-$ . Olsen and Burnelle<sup>9</sup> have made theoretical calculations of the geometry and electronic structure of the ground and lower excited states of this ion. The formation of the ion in the gas phase has been studied using drift tube mass spectrometers<sup>10-13</sup> and a flowing afterglow.<sup>14</sup> Two measurements<sup>15,16</sup> of the photodetachment of  $\text{CO}_3^-$  have been recently reported. In our studies of the photodissociation of  $\text{CO}_3^-$  in the gas phase,<sup>17,18</sup> we have observed behavior apparently characteristic of a predissociating excited state. In this paper we present the results of a more detailed experimental investigation of this state, and attempt to find the description of  $\text{CO}_3^-$  most consistent with all the available evidence.

The experiments were performed using a drift tube mass spectrometer,<sup>17,18</sup> an argon-ion laser, and a tunable dye laser. The  $\text{CO}_3^-$  ions, formed by reaction between  $\text{O}^-$  and  $\text{CO}_2$ , drift under the influence of a weak applied electric field toward an extraction aperture. The pressure of the  $\text{CO}_2$  gas in the drift region was typically 0.050 torr for these experiments. The ratio of

the electric field strength to the neutral-gas density,  $E/N$ , was chosen so that the directed drift velocity was only about one-tenth the mean thermal speed of the ions and gas molecules at room temperature. Thus, the ions experience many thermalizing collisions following their production. Just before passing through the extraction aperture, the ions intersect the intracavity photons of the dye laser, which is chopped at 100 Hz. The ions that pass through the extraction aperture are mass selected by a quadrupole mass spectrometer and individually detected by an electron multiplier. By counting these ions for alternate periods when the laser is on and off, we can determine the cross section for the loss of a particular ion species due to photon interaction, i.e., the total photodestruction cross section. Tuning the mass spectrometer to the appropriate mass permits identification of photofragment ions resulting from the photodissociation.

## II. PHOTODISSOCIATION SPECTRUM

We have measured the absolute photodestruction cross section for the process



using continuously tunable radiation with a  $0.5 \text{ \AA}$  bandwidth over the range from 6940 to  $5270 \text{ \AA}$ , and at seven discrete wavelengths of the argon-ion laser between 5287 and  $4579 \text{ \AA}$ . This cross section is presented in Fig. 1



as a function of photon energy. Some of these results were presented in Refs. 17 and 18, where we discussed in some detail experimental tests which established that the only important destruction process occurring is the single photon photodissociation represented by Eq. (1). Thus, photodetachment, multiple photon processes, and collisional dissociation or detachment do not contribute significantly to the cross section presented in Fig. 1. If the  $\text{CO}_3^-$  ions in reaction (1) have a thermal distribution of internal states, the structure observed in Fig. 1 should reflect transitions to various vibrational modes of one or more predissociating  $\text{CO}_3^-$  electronic states.

In earlier work,<sup>17,18</sup> we were able to conclude that the effect of vibrational excitation in the reactant  $\text{CO}_3^-$  molecule on either the magnitude or shape of the cross section was negligible at photon energies above 1.94 eV. Near the threshold for dissociation, however, the cross section should be particularly susceptible to any contributions from vibrational excitation in the  $\text{CO}_3^-$  at the time of photon absorption. The peaks in Fig. 1 near 1.80 and 1.85 eV might be especially suspected of originating from excited  $\text{CO}_3^-$  since they occur at relatively low photon energies. Unfortunately, the poorly defined peak near 1.80 eV could not be studied in detail owing to the small size of its cross section and the lack of photon intensity at these energies. The cross section at this energy may therefore originate from vibrationally excited  $\text{CO}_3^-$ . However, detailed studies of the peaks at 1.85 eV and higher energies, which are discussed

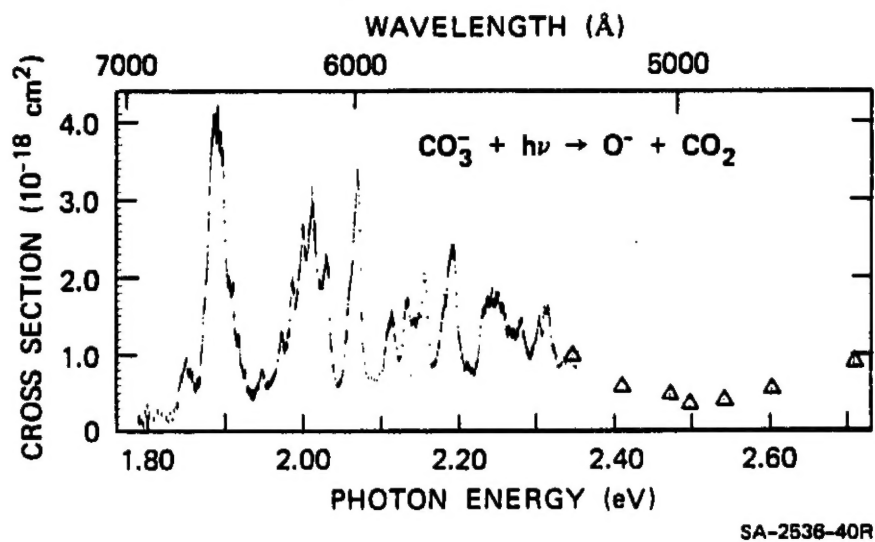


Figure 1. Photodissociation cross section of  $\text{CO}_3^-$  as a function of both photon energy and wavelength. The data shown as points were obtained using a tunable dye laser with a resolution of approximately 0.5 Å. The triangles are data taken at the discrete lines of the argon ion laser.

in the remainder of this section, show clearly that the main structure in Fig. 1 originates from ions in their ground vibrational levels.

The parent  $\text{CO}_3^-$  is formed by the reaction



We have previously<sup>17</sup> observed variations in the magnitude of the photodissociation cross section at 2.41 eV (5145 Å), which we attributed to vibrational excitation in the initial production of  $\text{CO}_3^-$  and to an increase in the photodissociation cross section at this energy with increasing vibrational excitation of the  $\text{CO}_3^-$  ion. We further showed that, at a  $\text{CO}_2$  pressure of 0.050 torr, an E/N of 10 Td ( $1 \text{ Td} = 10^{-17} \text{ V cm}^2$ ), and a drift distance of 10 cm or greater, the photodissociation cross section was constant, indicating that the initial vibrational excitation had been relaxed through collisions with the  $\text{CO}_2$  molecules in the drift region. Thus, under these conditions, the ions were essentially in thermal equilibrium with the gas molecules at room temperature.

If the photoabsorption occurring at 1.85 eV (6700 Å) originates from an excited level of the ground state, we would expect the observed photodissociation cross section in the region of this peak to increase under conditions that favored higher vibrational excitation in the ground state. One such condition is a short drift distance, so that the vibrationally excited  $\text{CO}_3^-$  ions produced by reaction (2) have fewer deexciting collisions before entering the laser beam. The cross section at 1.85 eV was measured for drift distances from 5 to 30 cm. Over this

range the number of collisions that a  $\text{CO}_3^-$  ion formed in the source underwent before intersecting the photon beam varied from approximately 200 to 1200. The actual increase was even greater, since for a drift distance of 5 cm approximately half the  $\text{CO}_3^-$  ions intersecting the laser beam are formed outside the source along the drift path preceding the laser beam, while for a drift distance of 30 cm essentially all the observed  $\text{CO}_3^-$  ions are formed 20 cm or more away from the laser beam. At 2.41 eV, under these same conditions, we observed a cross section for a 5-cm drift distance that was about 50% greater than that for a 15-cm drift distance. At 1.85 eV, however, no variation was observed in the cross section with drift distance, indicating either that this peak does not originate from a vibrationally excited level or that the collisional deexcitation cross section for such an excited level is less than  $10^{-18} \text{ cm}^2$ . Reasons for the apparent dependence of the cross section at 2.41 eV on the vibrational temperature of the  $\text{CO}_3^-$  ground state are not yet understood, but they do not affect the conclusions of this paper.

A second condition for enhancing the vibrational excitation in a  $\text{CO}_3^-$  ion when it interacts with the laser is to increase  $E/N$  in the drift region so that the ions have a mean kinetic energy<sup>19</sup> substantially above thermal (300°K) energy. This should have two effects: the deexcitation of any vibrational excitation produced in the formation of the  $\text{CO}_3^-$  may be reduced, and the increased average collision energy should enhance the parent ion vibrational excitation. Thus an increase in  $E/N$  will tend to

increase the temperature of the ions, although it is unlikely that the kinetic, vibrational, and rotational energies at any high E/N can be described by a single temperature. The photodissociation cross section at 1.85 eV was measured for E/N values from 10 to 150 Td, corresponding to mean center-of-mass kinetic energies ranging from essentially thermal energy (0.4 eV) to 0.13 eV, as calculated from the measured drift velocities using the Wannier relation.<sup>19</sup> At the higher E/N values, collisions between  $\text{CO}_3^-$  and  $\text{CO}_2$  were energetic enough to cause substantial vibrational excitation of the  $\text{CO}_3^-$ . At 2.41 eV (5145 Å), we again observed<sup>17</sup> a significant increase in the photodissociation cross section over this range of E/N. However, at 1.85 eV the cross section was observed to remain constant over this entire range of E/N values.

Thus, the photodissociation cross section at 1.85 eV appears to be independent of both the number of collisions and their energy, under conditions where significant dependencies were observed at 2.41 eV. This independence strongly indicates that the peak at 1.85 eV does not originate from a vibrationally excited level of the parent  $\text{CO}_3^-$ .

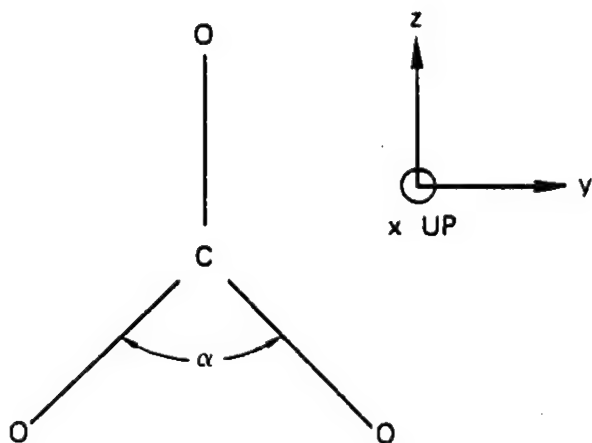
### III. VIBRATIONAL FREQUENCIES OF THE EXCITED STATE

The complexity of the structure and the close spacing of the peaks shown in Fig. 1 indicate that the transitions observed are to vibrational levels above the ground vibrational level of the excited electronic state. It can further be deduced that, near the dissociation energy of  $\text{CO}_3^-$ ,

substantial vibrational excitation of the excited state is needed to facilitate the dissociation.

Experiments in  $\text{KHCO}_3$  crystals<sup>4-6</sup> and in an argon matrix<sup>7</sup> have concluded that the ground state  $\text{CO}_3^-$  in these environments has  $C_{2v}$  symmetry, as shown in Fig. 2. Calculations for the free ion<sup>9</sup> also predict a  $C_{2v}$  geometry, with the unique angle  $\alpha$  less than  $120^\circ$ . At the threshold for dissociation, this molecule must break up into  $\text{O}^-$  and  $\text{CO}_2$ , with no excess kinetic or internal energy. The energy required to dissociate  $\text{CO}_3^-$  directly into  $\text{O}^-$  and  $\text{CO}_2$  bent at  $120^\circ$  has been calculated<sup>20</sup> to be between 1.2 and 2.5 eV greater than the adiabatic dissociation threshold at which the  $\text{CO}_2$  fragment is produced in its linear ground state. Consequently, over the range of measurements presented in Fig. 1, the dissociation of  $\text{CO}_3^-$  requires a substantial change in the geometry of the molecular ion. Such a change could result from the excitation of bending mode vibrations in the excited electronic state.

We therefore searched for vibrational spacings characteristic of the excited state that could explain the observed structure. The search was confined to the range 500 to  $2500\text{ cm}^{-1}$ , since vibrational spacings for similar molecules<sup>21</sup> lie in this range. It was found that three frequencies,  $990\text{ cm}^{-1}$ ,  $1470\text{ cm}^{-1}$ , and  $880\text{ cm}^{-1}$ , give reasonable identifications of nearly all the observed peaks if the ground vibrational level of the excited electronic state is assumed to be  $1.520 \pm 0.002\text{ eV}$  ( $12260 \pm 10\text{ cm}^{-1}$ ) above the ground level of the ground state. The peaks in Fig. 3 identified



SA-4239-11

Figure 2. Geometry of the ground state  $\text{CO}_3^{2-}$  ion having  $\text{C}_{2v}$  symmetry, showing the orientation of its coordinate system.

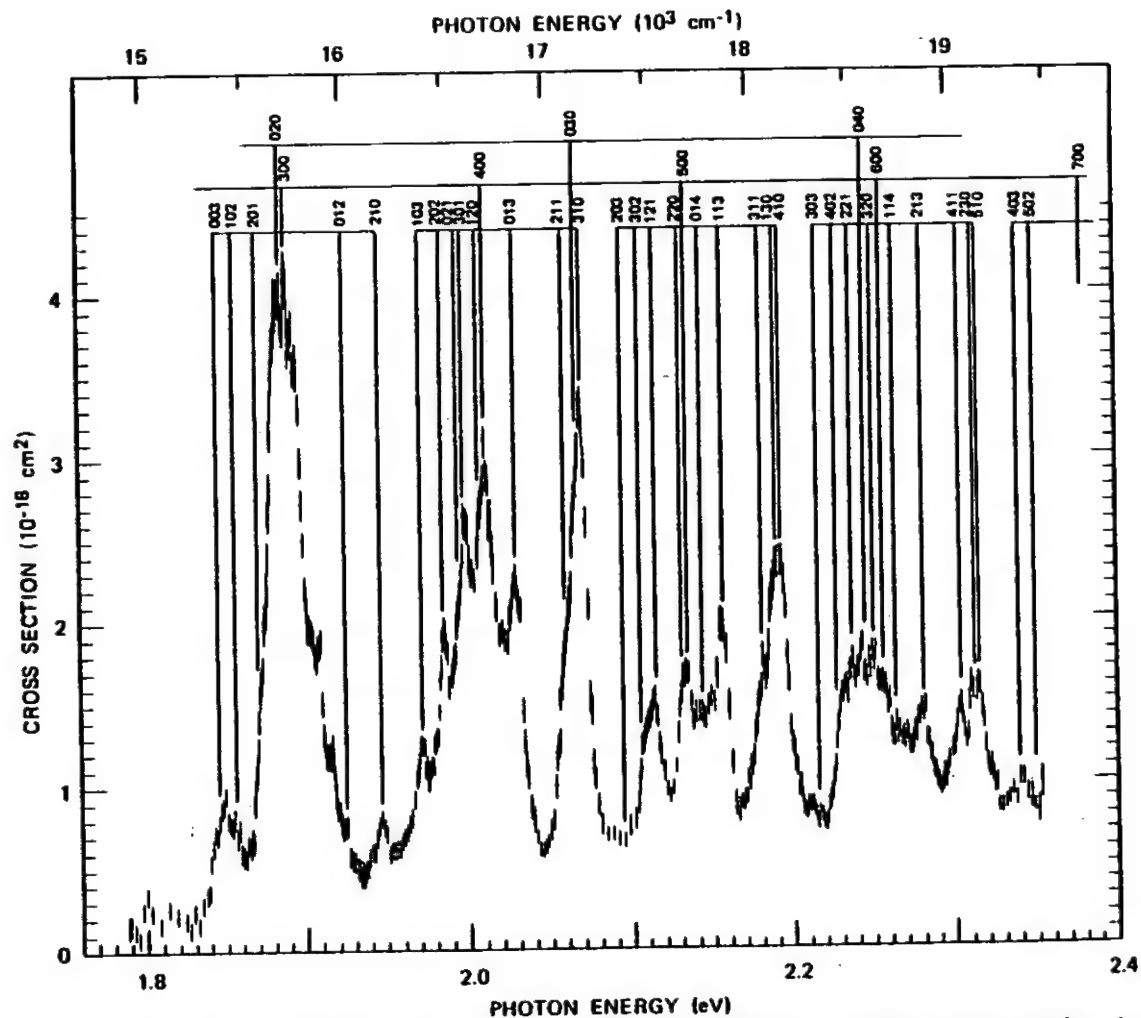


Figure 3. Photodissociation cross section of  $\text{CO}_2^-$  as a function of photon energy showing the assignment of transitions to three vibrational modes of the  $1^2A_1$  excited state from the ground vibrational levels of the  $1^2B_2$  state. The origin of the  $1^2A_1$  state is at  $1.520 \pm 0.002$  eV, and the vibrational modes are found to have frequencies of 990, 1470, and  $880 \text{ cm}^{-1}$ , respectively.



according to this scheme are labelled with a set of three numbers,  $ijk$ , indicating  $i$  units of the  $990\text{ cm}^{-1}$  vibration,  $j$  of the  $1470\text{ cm}^{-1}$  vibration, and  $k$  of the  $880\text{ cm}^{-1}$  vibration. The spectrum can be viewed as a series of groups, each subsequent group obtained by adding  $990\text{ cm}^{-1}$  to the energy of each peak in the preceding group. Superimposed on this is a progression in the  $1470\text{ cm}^{-1}$  vibration. The small peak at  $1.80\text{ eV}$  and the structure on the side of the large peak at  $1.89\text{ eV}$  are not explained by this scheme, but may arise from other vibrational levels of the excited state or from vibrationally excited levels of the ground state, as mentioned earlier.

It is difficult to identify these vibrational spacings with any specific three of the six vibrational modes of  $\text{CO}_3^-$ . However, since dissociation near the threshold requires such a large change in the angle  $\alpha$ , it is suggested that all these vibrational spacings correspond to bending modes of the excited state. We have studied selected regions of the  $^{13}\text{CO}_3^-$  photodissociation spectrum and find only a small isotope shift ( $9 \pm 3\text{ cm}^{-1}$  per vibrational quantum) for the peaks assigned to the  $1470\text{ cm}^{-1}$  vibration, and no detectable shift for the others. In the IR spectrum of the  $\text{CO}_3^-$  ground electronic state, Jacox and Milligan<sup>7</sup> observed shifts of  $33$  and  $42\text{ cm}^{-1}$ , respectively, for the  $1307$  and  $1494\text{ cm}^{-1}$  vibrational quanta; they identified these shifts as the two carbon-oxygen stretching fundamentals. The small shifts observed here, however, are more consistent with bending mode characteristics.

#### IV. IDENTIFICATION OF THE EXCITED STATE

The expected electron configurations of the ground and first four excited states of  $\text{CO}_3^-$  are discussed in some detail in Refs. 4, 8, and 9. The ground state is generally agreed to be a  $1^2B_2$  state, and both XHMO and INDO calculations<sup>9</sup> predict that the odd electron is in a  $4b_2$  orbital, which is largely antibonding for the two symmetry-equivalent oxygen atoms. The lowest lying excited states are  $2^2B_2$ ,  $1^2A_1$ ,  $1^2B_1$ , and  $1^2A_2$ . There should thus be four low-lying transitions:

$$2^2B_2 - 1^2B_2 \quad \text{Z polarized} \quad (3a)$$

$$1^2A_1 - 1^2B_2 \quad \text{Y polarized} \quad (3b)$$

$$1^2B_1 - 1^2B_2 \quad \text{forbidden} \quad (3c)$$

$$1^2A_2 - 1^2B_2 \quad \text{X polarized} \quad (3d)$$

for which the polarization of the radiation absorbed or emitted is given with respect to the coordinate system in Fig. 2.

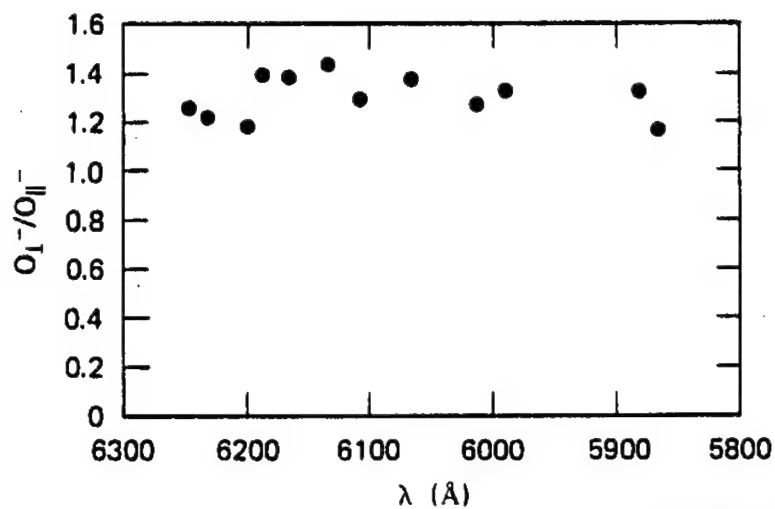
Transitions (3c) and (3d) are degenerate for  $D_{3h}$  symmetry, and since (3c) is dipole forbidden, (3d) might be expected to be weak. Transitions (3a) and (3b) are also degenerate for  $D_{3h}$ , but strongly allowed. Chantry et al.<sup>4</sup> attributed absorption bands (polarized in the plane of the ion) at  $5300 \text{ \AA}$  in  $\text{CO}_3^-$  and at  $6100 \text{ \AA}$  in the isoelectronic molecule  $\text{NO}_3$  to either transition (3a) or (3b), while assigning a transition at  $3280 \text{ \AA}$  for  $\text{NO}_3$  to (3d). The calculations of Olsen and Burnelle<sup>9</sup> predict transition (3a) to lie lowest, and that this transition is unlikely to result in a substantial change in the geometry of the system.

The calculations also predict that transition (3b) is next in energy and probably very close to (3a). Further, this transition should result in a substantial change in the geometry of the system, particularly in the angle  $\alpha$ , which would produce a photoexcitation spectrum well developed in bending mode structure. It appears reasonable from these calculations that, after a vertical transition to the  $1^2A_1$  state at the ground state equilibrium value of  $\alpha$  ( $110^\circ$  in the XMO calculation,  $82^\circ$  in the INDO), the molecule can undergo bending vibrations during which the angle  $\alpha$  approaches  $180^\circ$ . Since the  $2^2B_2 - 1^2B_2$  vertical transition should not substantially change  $\alpha$ , identification of the observed vibrational structure in the photodissociation cross section with this  $1^2A_1$  state appears most reasonable.

One way to distinguish between transitions (3a) and (3b) in our experiment is by the dependence of the detected  $O^-$  photofragment current on the orientation of the linearly polarized laser beam. The geometry of our apparatus<sup>17</sup> is such that photofragments ejected along the axis of the drift tube will be detected with higher efficiency than those ejected perpendicular to this axis. Of course, since the photon-ion interaction occurs in the relatively high pressure drift region, subsequent collisions may decrease the observed polarization effect. However, at the pressure of 0.050 torr at which the experiments reported here were performed, the ions can undergo on the average only three or four collisions before detection. We therefore attempted to observe a polarization effect on the detection efficiency of the  $O^-$  photofragments.

The results of this experiment are presented in Fig. 4, where the ratio of the detected  $O^-$  photofragment currents (normalized to the same photon flux) for the radiation polarized perpendicular and parallel to the drift tube axis is plotted versus wavelength. For transition (3a), we would expect the ratio  $(O_{\perp}^-/O_{\parallel}^-)$  to be less than 1; for transition (3b), it should be greater than 1. The result is clearly  $(O_{\perp}^-/O_{\parallel}^-) > 1$ , favoring the assignment of transition (3b). We should point out that transition (3d) would also be expected to yield  $(O_{\perp}^-/O_{\parallel}^-) > 1$ , but other evidence already discussed indicates that the state responsible for the observed structure is not the  $1^2A_2$ .

We thus conclude that the state responsible for the structure observed in the photodissociation cross section is the  $1^2A_1$ , which has its origin 1.520 eV ( $12260\text{ cm}^{-1}$ ) above the origin of the ground state and has three vibrational modes with energies of  $990\text{ cm}^{-1}$ ,  $1470\text{ cm}^{-1}$ , and  $880\text{ cm}^{-1}$ . All three of these vibrations probably represent bending modes of the ion in this state. Stretching modes may occur in the absorption spectrum, but may appear only weakly or not at all in the dissociation spectrum.



SA-4239-12

Figure 4. Ratio of the  $O_1^-$  photofragment ions detected when the electric vector of the laser was perpendicular to the  $CO_3^-$  drift velocity to those  $O_1^-$  photofragment ions detected when the electric vector was parallel to the  $CO_3^-$  drift velocity, plotted as a function of wavelength.

## V. OTHER OBSERVATIONS

The absolute cross sections presented in Fig. 1 were determined by observing the disappearance of  $\text{CO}_3^-$ , as discussed in Refs. 16 and 17. We have also observed<sup>17,18</sup> the appearance of  $\text{O}^-$  photofragments over the same range of photon energies. Because of the polarization effects discussed in the previous section, and other possible detector discrimination effects, it is not straightforward to relate the observed  $\text{O}^-$  photofragment current directly to the absolute photodissociation cross section.

Between 1.97 and 2.16 eV, the number of  $\text{O}^-$  photofragments detected was in excellent agreement<sup>18</sup> with that expected from the cross section as determined from the disappearance of  $\text{CO}_3^-$ . This was consistent with our assignment of the structure in this region to a perpendicular transition to the  $1^2\text{A}_1$  state. Between 2.41 and 2.59 eV, however, the  $\text{O}^-$  photofragment current exhibited<sup>17</sup> behavior substantially different from that of the photodestruction cross section. In particular (see Figures 2 and 3 of Ref. 17), photofragments for wavelengths between 2.53 and 2.71 eV were collected with much higher efficiency than those for wavelengths between 2.41 and 2.53 eV when the polarization of the laser beam was oriented perpendicular to the drift tube axis. One possible explanation for this effect, proposed in Ref. 17, is that the two wavelength regions correspond to photodissociation from two excited states of different symmetry. In this model, the 2.41-2.53 eV region would correspond to a parallel

transition since the photofragments are not collected efficiently, while the 2.53-2.71 eV region would correspond to a perpendicular transition, such as in the 1.97-2.16 eV region.

This explanation fits well with transitions (3a) and (3d). Theory<sup>9</sup> predicts that the  $2^2B_2$  state lies below the  $1^2A_2$  and that transition (3d) would occur at 2.7 eV. The polarization characteristics of transitions to these states are such that (3a) is a parallel transition, whereas (3d) is perpendicular. Thus it is possible that the photodissociation observed between 2.32 and 2.53 eV arises primarily from transition (3a) and that the photodissociation between 2.53 and 2.71 eV arises from (3d). Recent work by Vestal, Mauclaire, and Futrell<sup>22</sup> indicates that the photodissociation cross section has a maximum near 2.7 eV. This may be fortuitous agreement with theoretical prediction for transition (3d), but it does support the suggestion that the photodissociation between 2.53 and 2.71 eV is due primarily to transition (3d).

These conclusions regarding the assignment of transitions (3a) and (3d) are only tentative. They can be tested by further studies of the polarization and wavelength dependence of the cross section. Photofragment energy distributions<sup>23,24</sup> should also be studied to fully characterize these excited states.

## VI. BOND ENERGY AND ELECTRON AFFINITY

The photodissociation of  $\text{CO}_3^-$  is initiated by photoabsorption, which is a "vertical" transition from the ground state equilibrium configuration of the ion. The threshold for photodissociation can therefore be only an upper limit to the adiabatic dissociation limit or true  $\text{CO}_2\text{-O}^-$  bond energy,  $D(\text{CO}_2\text{-O}^-)$ . As shown in Fig. 3, we observe a strong dissociation peak at 1.85 eV, but note that dissociation also occurs weakly at 1.8 eV and possibly at even lower energies. Since our studies show that the 1.85 eV peak is not influenced by vibrational excitation of the ground  $\text{CO}_3^-$  electronic state, we regard 1.85 eV as an upper limit to  $D(\text{CO}_2\text{-O}^-)$ .

On the other hand, from the exothermicity of the reaction



obtained from the equilibrium constant, Ferguson, Fehsenfeld, and Phelps<sup>25</sup> have determined a lower limit of  $2.0 \pm 0.2$  eV for the bond energy  $D(\text{CO}_2\text{-O}^-)$ . We conclude that the bond energy  $D(\text{CO}_2\text{-O}^-)$  must in fact be very close to 1.80 eV. Thus, the range  $1.8 \pm 0.1$  eV seems almost certain to encompass  $D(\text{CO}_2\text{-O}^-)$ .

Given this value of the bond energy, the electron affinity of  $\text{CO}_3$  can be calculated from

$$\text{EA}(\text{CO}_3) = D(\text{CO}_2\text{-O}^-) + \text{EA}(\text{O}) - D(\text{CO}_2\text{-O}^-) \quad . \quad (5)$$

Using  $\text{EA}(\text{O}) = 1.462$  eV<sup>26</sup> and  $D(\text{CO}_2\text{-O}) = 0.4 \pm 0.2$  eV,<sup>27</sup> we obtain

$\text{EA}(\text{CO}_2) = 2.9 \pm 0.3$  eV. This value is consistent with our previous



conclusion<sup>17</sup> that the primary photodestruction mechanism at 2.71 eV (4579 Å) is photodissociation, not photodetachment. It is in conflict with the value of 1.8 eV for the electron affinity reported by Burt,<sup>15</sup> but it is now clear that photodissociation, not photodetachment, produced the photodestruction observed in his experiment. Hong, Woo, and Helmy<sup>16</sup> recently reported a measurement of the vertical detachment energy of  $\text{CO}_3^-$ , yielding a threshold of  $2.69 \pm 0.1$  eV, which is consistent with that calculated from Eq. (5).

## VII. SUMMARY

The photodissociation cross section of  $\text{CO}_3^-$  ions having a 300°K distribution of internal states has been measured at wavelengths between 4579 and 6940 Å. The cross section exhibits detailed structure at photon energies between 1.85 and 2.35 eV, characteristic of transitions to vibrational levels of an excited electronic state that predissociates to form  $\text{O}^-$  and  $\text{CO}_2$ . The major features of the cross section are single photon absorptions from the ground vibrational levels of the  $\text{CO}_3^-$   $1^2\text{B}_2$  ground electronic state. The polarization dependence of the  $\text{O}^-$  photofragments supports identification of the predissociating state as the  $1^2\text{A}_1$ . Three vibrational modes of this state are identified, having frequencies of  $900\text{ cm}^{-1}$ ,  $1470\text{ cm}^{-1}$ , and  $880\text{ cm}^{-1}$ . The small isotopic shifts observed in these frequencies for  $^{13}\text{CO}_3^-$  suggest their assignment to bending modes.

On the basis of these vibrational assignments, the origin of the  $1^2A_1$  state is predicted to occur 1.520 eV above the ground state. The present observations, together with other measurements, show the  $CO_3^-$  dissociation energy,  $D(CO_2-O^-)$ , and the  $CO_3$  electron affinity to be  $1.8 \pm 0.1$  eV and  $2.9 \pm 0.3$  eV, respectively.

#### ACKNOWLEDGMENTS

We would like to acknowledge very useful discussions with Dr. David L. Huestis, and the participation of Dr. Joyce H. Ling in the experimental work. One of us (JTM) has also benefited from discussions with Professor Jean Durup and Dr. Sydney Leach of the Université de Paris-Sud, Orsay, France, during the writing of this article.

## REFERENCES

\*This research was jointly supported by the U.S. Army Research Office and by the National Science Foundation under Grant No. MPS75-10085.

†Address for the 1975-76 academic year: Laboratoire des Collisions Ioniques, Université de Paris-Sud, 91405 Orsay, France.

1. R. S. Narcisi, A. D. Bailey, L. Della Lucca, C. Sherman, and D. M. Thomas, *J. Atmos. Terr. Phys.* 33, 1147 (1971).
2. F. Arnold, J. Kissel, D. Krankowsky, H. Wieder, and J. Zahringer, *J. Atmos. Terr. Phys.* 33, 1169 (1971).
3. W. L. Nighan and W. J. Wiegand, *Phys. Rev. A* 10, 922 (1974).
4. G. W. Chantry, A. Horsfield, J. R. Norton, and D. H. Whiffen, *Mol. Phys.* 5, 589 (1962).
5. R. A. Serway and S. A. Marshall, *J. Chem. Phys.* 46, 1949 (1967).
6. Z. H. Top, S. Raxiel, Z. Luz, and B. L. Silver, *J. Mag. Resonance* 12, 102 (1973).
7. M. E. Jacox and D. E. Milligan, *J. Mol. Spec.* 52, 363 (1974).
8. A. D. Walsh, *J. Chem. Soc.* 2301 (1953).
9. J. F. Olsen and L. Burnelle, *J. Amer. Chem. Soc.* 92, 3659 (1970).
10. J. L. Moruzzi and A. V. Phelps, *J. Chem. Phys.* 51, 863 (1969).
11. D. A. Parks, *Trans. Faraday Soc.* 68, 627 (1972); 69, 198 (1973).
12. H. W. Ellis, R. Y. Pai, I. R. Gatland, E. W. McDaniel, R. Wernland, and M. J. Cohen, to be published.
13. J. T. Moseley, P. C. Cosby, and J. R. Peterson, *J. Chem. Phys.* 64, (1976), in press.
14. D. K. Bohme, D. B. Dunkin, F. C. Fehsenfeld, and E. E. Ferguson, *J. Chem. Phys.* 51, 863 (1969).
15. J. A. Burt, *J. Chem. Phys.* 57, 4649 (1972).

16. S. P. Hong, S. B. Woo, and E. M. Helmy, Bull. Am. Phys. Soc. 21, 170 (1976).
17. J. T. Moseley, P. C. Cosby, R. A. Bennett, and J. R. Peterson, J. Chem. Phys. 62, 4826 (1975).
18. P. C. Cosby and J. T. Moseley, Phys. Rev. Letters 34, 1603 (1975).
19. E. W. McDaniel and E. A. Mason, The Mobility and Diffusion of Ions in Gases (John Wiley and Sons, Inc., New York, 1973).
20. N. W. Winter, private communication.
21. G. Herzberg, Molecular Spectra and Molecular Structure III (Van Nostrand, Reinhold Company, New York, 1966).
22. M. L. Vestal, G. Mauclaire, and J. H. Futrell, 23rd Conference on Mass Spectrometry, Houston, Texas (1975).
23. J. B. Ozenne, D. Pham, and J. Durup, Chem. Phys. Lett. 17, 422 (1972).
24. N.P.F.B. van Assett, J. G. Maas, and J. Los, Chem. Phys. Lett. 24, 555 (1974); Chem. Phys. 5, 429 (1974).
25. E. E. Ferguson, F. C. Fehsenfeld and A. V. Phelps, J. Chem. Phys. 59, 1565 (1973).
26. H. Hotop and W. C. Lineberger, J. Phys. Chem. Ref. Data 4, 539 (1975).
27. S. W. Benson, private communication.

# DISTRIBUTION LIST

<u>No. of Copies</u>	<u>Organization</u>	<u>No. of Copies</u>	<u>Organization</u>
12	Commander Defense Documentation Center ATTN: DDC-TCA Cameron Station Alexandria, VA 22314	1	Director Defense Communications Agency ATTN: Code 340, Mr. W. Dix Washington, DC 20305
1	Director Institute for Defense Analyses ATTN: Dr. E. Bauer 400 Army Navy Drive Arlington, VA 22202	1	Commander US Army Materiel Development and Readiness Command ATTN: DRCDMA-ST 5001 Eisenhower Avenue Alexandria, VA 22333
2	Director Defense Advanced Research Projects Agency ATTN: STO, CPT J. Justice LTC W. A. Whitaker 1400 Wilson Boulevard Arlington, VA 22209	1	Commander US Army Aviation Systems Command ATTN: DRSAB-E 12th and Spruce Streets St. Louis, MO 63166
1	Director of Defense Research and Engineering ATTN: CAPT K. W. Ruggles Washington, DC 20301	1	Director US Army Air Mobility Research and Development Laboratory Ames Research Center Moffett Field, CA 94035
4	Director Defense Nuclear Agency ATTN: STAP (APTL) STRA (RAAE) Dr. C. Blank Dr. H. Fitz, Jr. DDST Washington, DC 20305	1	Commander US Army Electronics Command ATTN: DRSEL-RD Fort Monmouth, NJ 07703
2	DASIAC/DOD Nuclear Information and Analysis Center General Electric Co - TEMPO ATTN: Mr. A. Feryok Mr. W. Knapp 816 State Street P. O. Drawer QQ Santa Barbara, CA 93102	3	Commander/Director Atmospheric Sciences Laboratory US Army Electronics Command ATTN: Dr. E. H. Holt Mr. H. Ballard Dr. F. E. Niles White Sands Missile Range NM 88002
		1	Commander US Army Missile Command ATTN: DRSMI-R Redstone Arsenal, AL 35809

# DISTRIBUTION LIST

<u>No. of Copies</u>	<u>Organization</u>	<u>No. of Copies</u>	<u>Organization</u>
1	Commander US Army Tank Automotive Development Command ATTN: DRDTA-RWL Warren, MI 48090	2	Commander US Army Ballistic Missile Defense Systems Command ATTN: SSC-HS, H. Porter SSC-TET, E. Carr P. O. Box 1500 Huntsville, AL 35807
2	Commander US Army Mobility Equipment Research & Development Command ATTN: Tech Docu Cen, Bldg. 315 DRSME-RZT Fort Belvoir, VA 22060	1	HQDA (DACS-BMT) Arlington, VA 22209
1	Commander US Army Armament Command Rock Island, IL 61202	1	HQDA (DAEN-RDM, Dr. de Percin) Washington, DC 20314
2	Commander US Army Harry Diamond Labs ATTN: DRXDO-TI DRXDO-NP, F. Wimenitz 2800 Powder Mill Road Adelphi, MD 20783	1	Chief of Naval Research ATTN: Code 418, Dr. J. Dardis Department of the Navy Washington, DC 20360
1	Director US Army TRADOC Systems Analysis Agency ATTN: ATAA-SA White Sands Missile Range NM 88002	1	Commander US Naval Surface Weapons Center ATTN: Dr. L. Rutland Silver Spring, MD 20910
1	Commander US Army Nuclear Agency ATTN: Mr. J. Berberet Fort Bliss, TX 79916	1	Commander US Naval Electronics Laboratory ATTN: Mr. W. Moler San Diego, CA 92152
1	Commander US Army Research Office ATTN: Dr. A. Dodd P. O. Box 12211 Research Triangle Park NM 27709	3	Commander US Naval Research Laboratory ATTN: Dr. W. Ali Code 7700, J. Brown Code 2020, Tech Washington, DC 20375
		4	HQ USAF (AFNIN; AFRD; AFRDQ; AFTAC, COL C. Anderson) Washington, DC 20330
		2	AFSC (DLCAW, LTC R. Linkous; SCS) Andrews AFB Washington, DC 20334

# DISTRIBUTION LIST

<u>No. of Copies</u>	<u>Organization</u>	<u>No. of Copies</u>	<u>Organization</u>
5	AFGL (LKD, Dr. R. Narcisi; LKB, Dr. K. Champion, Dr. T. Keneshea, Dr. W. Swider; OPR, Dr. H. Gardiner) Hanscom AFB, MA 01730	2	Sandia Laboratories ATTN: Org 3141, Tech Lib Org 100, F. Hudson P. O. Box 5800 Albuquerque, NM 87115
1	Director National Oceanic and Atmospheric Administration ATTN: Dr. E. Ferguson US Department of Commerce Boulder, CO 80302	1	Pennsylvania State University Ionospheric Research Laboratory ATTN: Dr. L. C. Hale University Park, PA 16802
1	Director Brookhaven National Laboratory ATTN: Docu Sec 25 Brookhaven Avenue Upton, NY 11973	4	Stanford Research Institute ATTN: Dr. J. Peterson 333 Ravenswood Avenue Menlo Park, CA 94025
2	Director Los Alamos Scientific Lab ATTN: Lib Dr. W. Maier (Gp J-10) P. O. Box 1663 Los Alamos, NM 87544	1	State University of New York Department of Atmospheric Sciences ATTN: Dr. V. Mohnen Albany, NY 12203
1	Bell Telephone Laboratories, Inc Technical Report Service ATTN: Tech Rpts Specialist WH 5E-227 Whippany, NJ 07981	1	CIRES University of Colorado ATTN: Dr. A. W. Castleman Boulder, CO 80302
1	General Electric Company Valley Forge Space Technology Center ATTN: Dr. M. Bortner P. O. Box 8555 Philadelphia, PA 19101	2	University of Colorado Joint Institute for Laboratory Astrophysics ATTN: Dr. W. C. Lineberger Dr. A. V. Phelps Boulder, CO 80302
1	R&D Associates ATTN: Dr. F. Gilmore P. O. Box 3580 Santa Monica, CA 90403	1	University of Denver Denver Research Institute ATTN: Dr. R. Amme P. O. Box 10127 Denver, CO 82010
		1	University of Illinois Electrical Engineering Department Aeronomy Laboratory ATTN: Prof. C. Sechrist Urbana, IL 61801

# DISTRIBUTION LIST

<u>No. of Copies</u>	<u>Organization</u>
1	University of Minnesota, Morris Div of Science & Mathematics ATTN: Dr. M. N. Hirsh Morris, NM 56267
1	University of Pittsburgh Cathedral of Learning ATTN: Dr. M. A. Biondi 400 Bellefield Avenue Pittsburgh, PA 15213
1	University of Texas at El Paso Physics Department ATTN: J. Collins El Paso, TX 79902

## Aberdeen Proving Ground

Marine Corps Ln Ofc  
Dir, USAMSAA





